Enhancing Fire Resistance: A Thermal and Structural Optimization Approach for Fire Door Frame Using Numerical Simulation

Margarida Fernandes , Ana Araújo , João Silva * , Nelson Rodrigues , Senhorinha Teixeira , José Carlos Teixeira

Posted Date: 1 January 2026

doi: 10.20944/preprints202601.0047.v1

Keywords: fire doors; fire protection; finite element method (FEM); numerical optimization; thermal performance; structural integrity

 doi:10.20944/preprints202601.0047.v1

Article

Enhancing Fire Resistance: A Thermal and Structural Optimization Approach for Fire Door Frame Using Numerical Simulation

Margarida Fernandes [1], Ana Araújo [2], João Silva [1,2,*], Nelson Rodrigues [1], Senhorinha Teixeira [1] and José Carlos Teixeira [2]

[1] Centro ALGORITMI/LASI, University of Minho, 4800-058 Guimarães, Portugal
[2] Centro MEtRICs, University of Minho, 4800-058 Guimarães, Portugal
* Correspondence: js@dem.uminho.pt

Abstract

Fire resistance is a critical aspect of passive fire protection, particularly in door systems that must maintain integrity under extreme conditions. This paper presents the thermal and structural performance of a single-leaf sandwich fire door, with the goal of improving its fire resistance through numerical optimization. An initial numerical assessment identified the door frame as the thermally weakest component, guiding the subsequent optimization process. Then, a one-way coupled transient thermal–structural Finite Element Method (FEM) analysis was performed using ANSYS Mechanical to evaluate the influence of frame material, frame geometry, and insulation type and placement on the door–frame assembly when exposed to fire. Results show that the frame material plays a decisive role where aluminum alloys performed poorly, whereas wooden frames significantly reduced temperatures in both the door and frame by approximately 55% relative to the original configuration. Additional improvements were achieved by increasing frame thickness and placing rock wool within the thermal break, resulting in temperature reductions of 58.3% in the door and 57.3% in the frame. However, these thermal improvements had limited impact on structural deformation, which remained nearly unchanged.

Keywords: fire doors; fire protection; finite element method (FEM); numerical optimization; thermal performance; structural integrity

1. Introduction

Fire doors ensure resistance to fire and smoke and can prevent their spreading throughout external spaces in a building, making it possible to safeguard lives and goods in the event of a fire [1–3]. Only through certification can it be guaranteed that fire doors have the necessary fire resistance for the time required [4–6]. However, it is essential to improve their technical characteristics in order to achieve more demanding certification standards and strengthen their position in the market. In view of the work already carried out in this area, it is possible to highlight three simulation approaches that are mainly used: FEM, Computational Fluid Dynamics (CFD) and the coupling of the two.

FEM has been widely used to simulate the thermal and structural behavior of fire doors. For instance, Boscariol et al. [7,8] developed a numerical model using non-linear transient and steady-state thermal analyses with FEM to study the thermomechanical response. They concluded that steady-state analysis is satisfactory for thermal behavior, however increasing insulation reduces unexposed temperature while concurrently increasing door distortion and the frame-door gap. In a different perspective, D'Amore et al. [9] performed combined thermal and structural analyses, concluding that a transient model is necessary for accurately predicting temperature and distortion. In a subsequent study, they [10] used FEM to explore lighter insulation materials, finding them viable,

 doi:10.20944/preprints202601.0047.v1

though performance was significantly impacted by thermal bridges at the door edges. Kim et al. [11] used a 3D thermal model to develop a High Insulation Fire Door. Results showed that the best thermal performance was achieved by applying ceramic boards on the door leaves, positioning the gaskets as close as possible to the exterior and using a cavity-filled frame. Although the experimental validation showed a thermal performance 18% lower than predicted by the simulations, this discrepancy remained within acceptable limits. Khalifa et al. [12] optimized a fire door by inserting internal reinforcements with different geometries. A FEM model with coupled transient thermal-structural simulations was developed, showing that hat-omega stiffeners were the most effective in reducing deformations, with experimental data validating its accuracy.

CFD is also extensively applied to simulate the fire environment, gas flow, combustion and heat transfer phenomena influencing fire doors. In Leung et al. [13], a CFD analysis was carried out on a fire door subject to the standard temperature-time curve, with the objective to reproduce a fire resistance test. Convergence was achieved between the regions with highest and lowest temperature increases on the unexposed face. Tlili et al. [14] resorted to a CFD-based numerical approach to evaluate the influence of the location of a heat source inside a compartment under fire conditions. They found that the vertical position had the greatest impact on thermal stratification. Furthermore, through experimental data, it was proposed that an empirical correlation linking mass flow rate of air flowing through the door with the source positioning, enabling ventilation rates to be calculated without further simulations or tests. Iya et al. [15] conducted a study to assess the influence of the opening dimensions (ventilation level) on the power a diesel fuel releases inside a compartment. Based on experimental data and CFD numerical simulations, the authors concluded that the opening dimensions significantly influence the power generated inside the compartment, establishing ventilation as a fundamental aspect of fire behavior.

Alternatively, coupling CFD and FEM offers a comprehensive simulation framework to capture both the fire environment and the structural response of fire doors. Prieler et al. [16] expanded a previously developed model focused on multiphase heat transfer in porous gypsum and conducted a study based on coupled CFD-FEM simulations of gypsum-sheathed stud walls with an embedded steel door under fire exposure [17]. A model capable of predicting gaps between the wall and the door was achieved, demonstrating the potential of coupled simulation to anticipate critical functional failures in fire scenarios. While the previous work focused on wall systems with embedded doors, Prieler et al. [18] developed a CFD model for fire resistance tests that included gas-phase combustion and heat transfer in the specimen and validated it experimentally. Following this, the authors extended their approach by coupling the CFD thermal results with a structural FEM analysis to investigate the mechanical behavior of a three-parted steel door during fire resistance tests [19]. Results demonstrated computational efficiency and the ability to accurately predict the thermal and structural behavior of the metal door. De Boer et al. [20] used a two-way CFD-FEM coupling approach to analyze the behavior of a self-supporting sandwich panel façade system when subjected to fire. This type of coupling proves to be more reliable compared to one-way coupling, as it considers the mutual dependency between fire development and the mechanical response of the structure and vice versa, allowing changes in one domain to directly affect the other [21]. The model confirmed the thermal bowing phenomenon, which delayed the failure of the most critical screws through stress redistribution.

Based on the foregoing, this work first assesses the thermal and structural behavior of a single-leaf sandwich door under fire exposure, establishing the frame as the most critical component. Subsequently, the study further focuses on numerically optimizing the frame technical characteristics to enhance the overall fire door performance. Although a coupled CFD-FEM approach offers more detailed analyses, the lack of information about the furnace inlet and outlet made it impossible to use. Thus, with the main objective of optimizing a fire door frame when under fire exposure, the present work developed a FEM model using Ansys Mechanical. To support this optimization goal, critical parameters affecting fire resistance, such as frame material and geometry, insulation placement within the frame, and insulating materials were investigated.

 doi:10.20944/preprints202601.0047.v1

2. Materials and Methods

2.1. Baseline Model: Geometry and Materials

The baseline model under analysis (Figure 1) consists of a single-leaf sandwich door with the following dimensions: 1000 mm in width, 2103 mm in height and 50 mm in thickness. Being a sandwich panel, this door is composed of Halspan along its thickness (44 mm thick) and phenolic panels (3 mm thick) on both faces. It is also worth noting that the door has a phenolic border around its perimeter (18 mm thick).

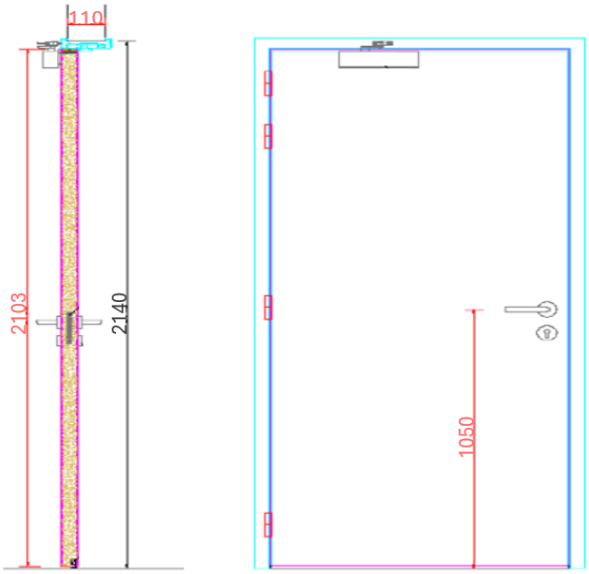

Figure 1. Single-leaf sandwich door (in dark blue) and frame (in light blue) assembly: a) cross-section view and b) front view (dimensions in mm).

As far as the frame (Figure 2) is concerned its material is the aluminum alloy EN AW 6063-T5. In addition, like most frames, it has rubbers in the door stop area, as well as around the frame in direct contact with the wall. In the fire resistance test of the fire door prototype that was carried out, insulation material was placed inside the frame, both in the door stop area (Halspan) and at its ends (Phenolic). Two steel plates (1 and 2 mm thick) were also fixed to the frame in the area between the frame and the wall, to provide structural resistance to the frame in the event of high temperatures and consequent failure of the aluminum. However, for modeling purposes, a single 1.5 mm metal sheet was considered.

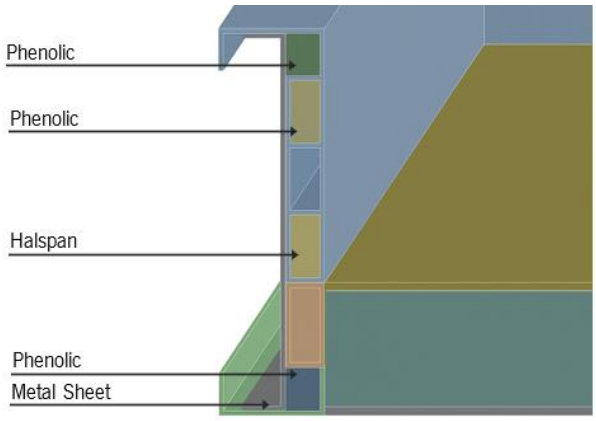

Figure 2. Door frame under analysis in its tested configuration.

 doi:10.20944/preprints202601.0047.v1

It should be noted that the door includes hardware, such as the handle, hinges, key entry, lock, door closer and door seal. Finally, like any door, this one also has gaps, both between the door and the frame (3 - 5 mm) and between the door and the floor (7 - 10 mm).

2.2. Governing Equations

As previously mentioned, given the lack of information regarding the oven inlet and outlet conditions, the CFD approach, as well as its coupling with Mechanical could not be pursued. Therefore, the numerical analyses were carried out using FEM alone.

As far as the physical model equations of this problem are concerned, they include both thermal and structural equations where the thermal solution was used as an input for structural analysis.

2.2.1. Thermal Equations

The numerical analysis of heat transfer within the fire door is governed by the first law of thermodynamics, which states that thermal energy is conserved. By focusing on the finite element formulation, the discrete equation governing the transient heat transfer phenomenon in the element can be described by Equation 1:

$$[C_e^t]\{\dot{T}_e\} + ([K_e^{tm}] + [K_e^{tb}] + [K_e^{tc}])\{T_e\} = \{Q_e^f\} + \{Q_e^c\} + \{Q_e^g\} \quad (1)$$

where $[C_e^t]$ represents the element specific heat matrix, $\{\dot{T}_e\}$ is the nodal temperature vector of element, $[K_e^{tm}]$ refers to the mass transport conductivity matrix of the element, $[K_e^{tb}]$ is the element diffusion conductivity matrix, $[K_e^{tc}]$ is the element convection surface conductivity matrix, $\{Q_e^f\}$ represents the mass flux vector of the element, $\{Q_e^c\}$ is the element convection surface heat flow vector and $\{Q_e^g\}$ refers to the heat generation load of the element [22].

2.2.2. Structural Equations

Finite Element Analysis (FEA) is based on the principle of virtual work, promoting the discretization of a structure into finite elements, as well as the analysis of their behavior through the application of virtual displacements [23]. This principle establishes that an infinitesimal virtual change in internal deformation energy must be compensated by an equivalent variation in external work due to the applied loads [24]. This enables the formulation of equilibrium equations and the resolution of complex structural problems when considering the interaction between forces and displacements [23]. The principle of virtual work can then be mathematically expressed by Equation 2 [24]:

$$([K_e] + [K_e^f])\{u\} - \{F_e^{th}\} = [M_e]\{\ddot{u}\} + \{F_e^{pr}\} + \{F_e^{nd}\} \quad (2)$$

here $[K_e]$ represents the element stiffness matrix, $[K_e^f]$ is the element foundation stiffness matrix, $\{u\}$ is related to the nodal displacements, $\{F_e^{th}\}$ is the element thermal load vector, $[M_e]$ is the element mass matrix, $\{\ddot{u}\}$ is the acceleration vector, $\{F_e^{pr}\}$ is the element pressure vector and $\{F_e^{nd}\}$ refers to the nodal forces applied to the element.

2.3. Initial and Boundary Conditions

The numerical model was divided into two parts: transient thermal and transient structural analyses. An initial condition in both simulations of a temperature of 22 °C was set for all the model components. In a real certification test both faces of the door are exposed to fire. Therefore, in the simulation scenario, they will be subjected to the normalized Temperature-Time curve according to the standard EN 13501-2 [6], given by Equation 3.

$$T = 345 \times \log_{10}(8t + 1) + T_{amb} \quad (3)$$

Here, T represents the temperature, t the time and T_{amb} refers to the ambient temperature. Thus, when the hinges are exposed to fire (Figure 3 a)), the face of the door facing the furnace is the one aligned with the frame. Conversely, when the hinges are not exposed to fire (Figure 3 b)), the face of

 doi:10.20944/preprints202601.0047.v1

the door turned toward the interior of the furnace is the one not aligned with the frame. In such cases, the frame has a greater surface area in contact with fire compared to the opposite face, therefore experiencing higher temperatures.

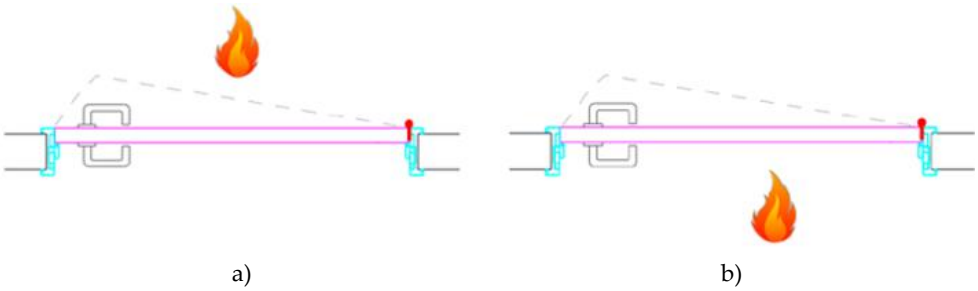

a) b)

Figure 3. Representative diagram of the door faces with a) hinges exposed to fire and b) unexposed hinges to fire.

In the other hand, a convective heat transfer coefficient varying over time is applied on the face unexposed to fire. Figure 4 shows the temporal evolution of the convective heat transfer coefficient, computed using an empirical correlation for the average Nusselt number in natural convection over a vertical flat plate.

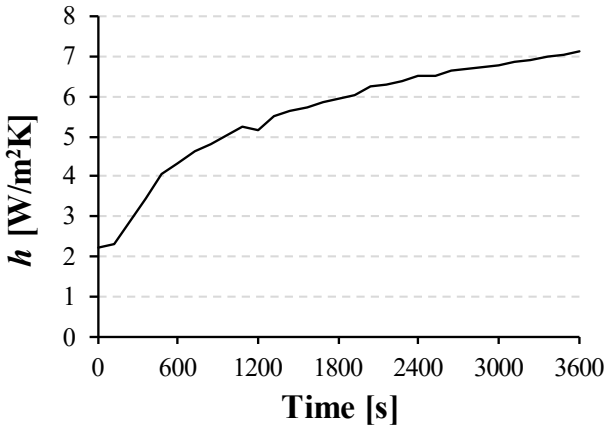

Figure 4. Time evolution of the convective heat transfer coefficient.

Despite the physical gap between the door and the frame, for thermal simulation purposes, a frictionless contact condition was defined with a conductance value of 10 W/(m²·K). Furthermore, a pure penalty method was employed to mitigate possible element interpenetration.

Regarding the transient structural simulation boundary conditions, appropriate constraints were established. A Fixed Support (represented in Figure 5) was placed on the internal face of the frame (the portion fitted into the wall) to simulate its embedding within the wall structure. Hardware components, such as hinges and locks, were fully constrained having had a null displacement applied in all directions, as they join and restrict the deformation of the door and frame. Conversely, the door bottom face (near the threshold) received a null displacement only at the *z*-axis (Figure 6) to prevent inward deformation. In contrast to the thermal simulation, the structural simulation does not consider the contact between the door and the frame, since they are not in direct contact.

 doi:10.20944/preprints202601.0047.v1

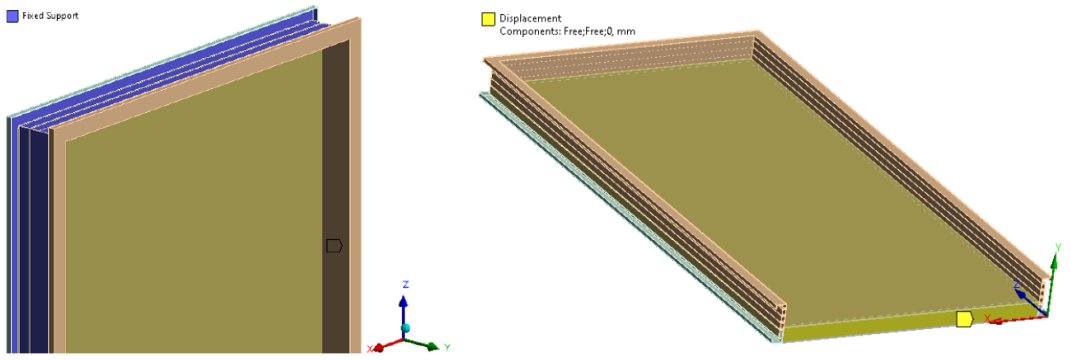

a) b)

Figure 5. Structural restrictions: a) fixed support applied to the interior part of the frame, and b) application of null displacement on the bottom face of the door along the *z*-axis.

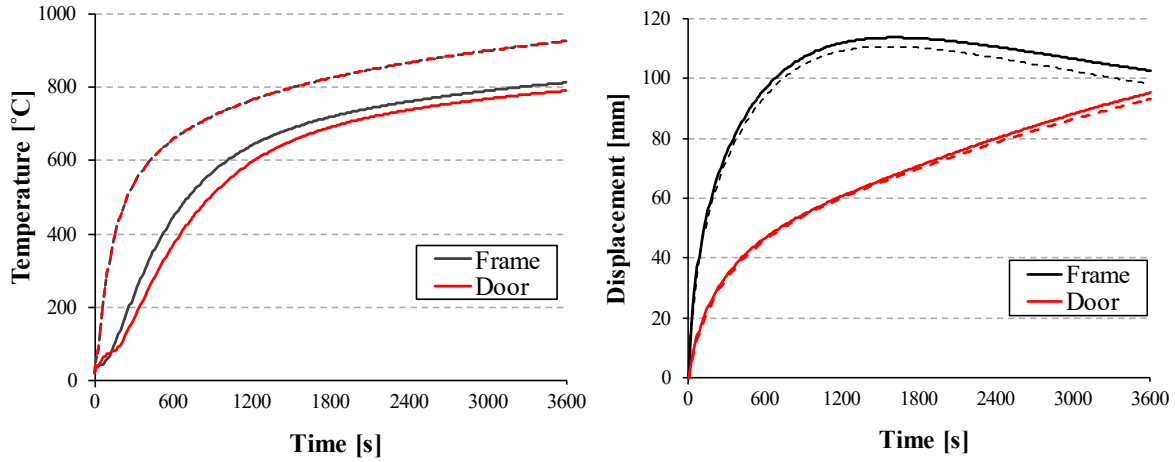

a) b)

Figure 6. a) Temperature evolution of the frame and door over time, considering both the exposed and unexposed hinges, and b) Displacement of the upper corner of the frame and door over time, considering both the exposed and unexposed hinges.

2.4. Simulation Setup

A uniform mesh with 21 154 elements was used for both the thermal and structural analyses to ensure direct compatibility with the results. In order to accommodate some geometric features, local variations in mesh density were necessary.

Regarding the Analysis Settings, these were kept common across both simulations, where 30 steps of 120 s for a total duration of 3600 s were defined. This 120 s step duration was defined to facilitate the stable implementation of the convective heat transfer coefficient, without compromising either result quality or the overall simulation time. Furthermore, Auto Time Stepping was deactivated. Instead, 10 sub-steps were defined per step, as this value demonstrated the best balance between result accuracy and computational cost. Lastly, the transfer of results was handled by linking the Thermal Solution to the Structural Setup, enabling the use of the Imported Body Temperature boundary condition. The complete simulation thus utilizes a one-way coupling approach, where thermal results directly influence the structural response.

3. Results and Discussion

3.1. Original Door-Frame Assembly

In order to establish a performance baseline and substantiate the structural optimization, the thermal and structural behavior of the original door-frame assembly is initially presented. Figures 8

 doi:10.20944/preprints202601.0047.v1

and 9 illustrate the temperature temporal evolution, both in the frame and the door, for both the exposed and unexposed hinges cases. After 3600 s, both the frame and door (Figure 6 a)) reached 925 °C for the unexposed hinges case, whilst for the exposed hinges the temperatures of the door and frame were 790 and 812 °C, respectively. This difference highlights the influence of the frame in the unexposed hinges case, a result consistent with the fact that, in such configuration, the frame has a greater surface area in contact with the fire compared to the opposite face, thus experiencing higher temperatures.

Regarding the door deformation results, they are quite similar both for the case of the exposed hinges and unexposed hinges. Furthermore, as expected, these results showed deformation of the upper and lower corners on the latch side towards the outside of the furnace, with the upper corner showing greater deformation over time, reaching a displacement of 113 mm in the case of the exposed hinges (Figure 6 b)). The graphs show a more accentuated growth of the deformation in the upper corner, this being justified by the proximity of this area to the frame along its entire edge, unlike what happens in the lower corner (Figure 6 b)). It is important to mention that some deformation was observed in the central area of the door, in this case towards the inside of the furnace and on a smaller scale than the deformations mentioned above.

It should be noted that these displacement values may be lower, especially in the case of the exposed hinges, due to the presence of the door stop in the frame.

Based on the thermal and deformation results of the door, a limitation in the simulation model is identified, since the temperature distribution does not fully explain the behavior observed in terms of deformation. Although, from a thermal point of view, the most severe scenario corresponds to the unexposed hinges, the highest levels of deformation were recorded in the case of the exposed hinges, highlighting a discrepancy between the simulated thermal effects and the predicted structural response. Despite this limitation, the thermal results unequivocally establish the frame as the most vulnerable component of the assembly, achieving the highest temperatures. Consequently, this study focuses on the structural optimization of the frame, given that the overall response of a fire door is determined by its most susceptible component. In addition to this, since the highest temperatures are recorded with the unexposed hinges, the subsequent analysis and optimization will focus exclusively on this configuration.

3.2. Optimization Methodology

Following the identification of the frame as the weakest link of the overall fire door, the study focuses on its optimization, where the influence of several design features on the global response is evaluated. These design features involve the material and geometry of the frame, as well as the insulation materials and its placement. The sequence of optimizations followed an iterative and sequential approach, where each subsequent design modification was based on the most effective result from the preceding analysis.

The numerical approach considered two distinct frame geometries (Figure 7). In these configurations, the frame has a simplified geometry and may appear with a metal sheet on its interior (Figure 7 a)) or with insulation up to the wall (Figure 7 b)). The insulation up to the wall represents an additional insulation which, replacing the sheet, can be placed within the frame.

To clearly define the insulation placement options, a diagram of the frame structure is presented in Figure 8. It is important to note the difference between Zones 5 and 5a, given that the former corresponds to the entire region marked in orange in Figure 8, including Zone 5a, and the latter refers specifically to the interior zone delimited by the dashed line, visible in the detail view of Figure 8. Thus, Zone 5 is referred to as “the entire thermal break,” while Zone 5a is referred to as “inside the thermal break”. The design configurations and variations studied are detailed in Table 1.

 doi:10.20944/preprints202601.0047.v1

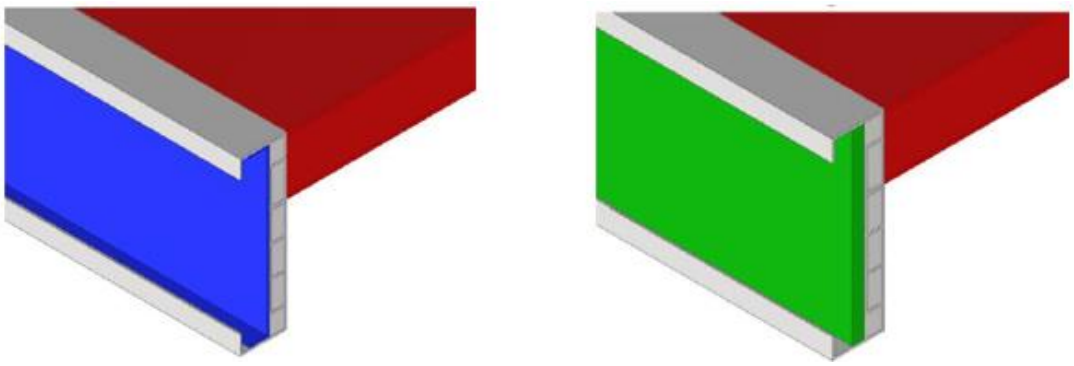

a) b)

Figure 7. Geometries used in the simulation process: a) metal sheet and b) insulation up to the wall.

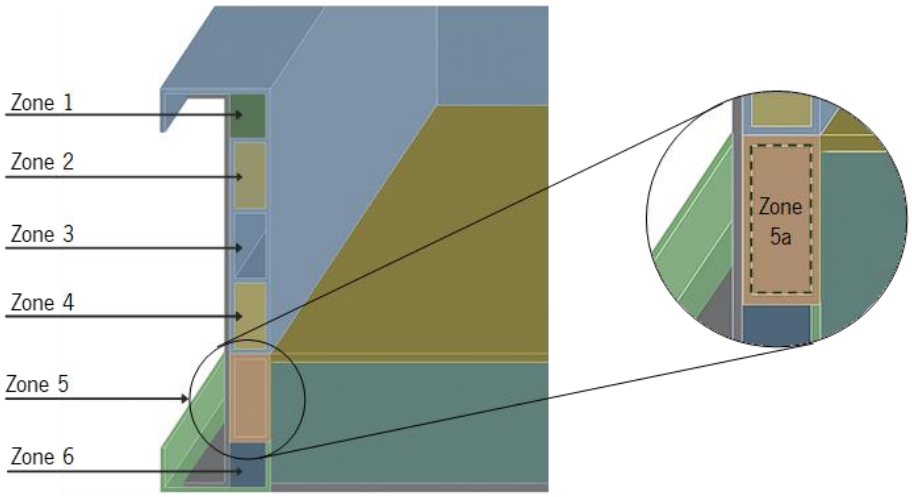

Figure 8. Schematic representation of the frame, indicating the zones considered for insulation placement.

Table 1. Design configurations and parameter variations for frame optimization.

Case Study	Numerical Analysis	Geometry	Materials
Frame Material	Aluminum alloy frame	Frame without steel sheet and insulations.	Halspan, phenolic, stainless steel and aluminum alloy.
	Stainless steel frame		Halspan, phenolic and stainless steel.
	Wood frame		Halspan, phenolic, stainless steel and wood.
Frame Geometry	With insulation up to the wall	Frame up to the wall with all insulation cavities filled.	Halspan, phenolic, stainless steel and wood.
	Only with the steel sheet	Frame with steel sheet with all insulation cavities filled.	
Insulating placement in the frame	Inside the thermal break (Zone 5a)	Frame up to the wall with varying insulation placements.	Halspan, phenolic, stainless steel, wood and rock wool.
	Across the entire thermal break (Zone 5 and 5a)		
	Near the door (Zones 5a and 6)		

 doi:10.20944/preprints202601.0047.v1

	At the frame boundaries (Zones 1 and 6)		
	At the frame insulations (Zones 2, 3, 4 and 5a)		
	All the frame insulation cavities (Zones 1, 2, 3, 4, 5 and 6)		
	Inside the thermal break and at the boundaries (Zones 1, 5a and 6)		
Insulating Materials	Rock wool	Frame up to the wall with insulation inside the thermal break.	Halspan, phenolic, stainless steel, wood and rock wool.
	Calcium silicate		Halspan, phenolic, stainless steel, wood and calcium silicate.
	Gypsum board		Halspan, phenolic, stainless steel, wood and gypsum board.
	Glass wool		Halspan, phenolic, stainless steel, wood and glass wool.
	Polyurethane foam		Halspan, phenolic, stainless steel, wood and polyurethane foam.
	Ceramic fiber		Halspan, phenolic, stainless steel, wood and ceramic fiber.

3.3. Assessment of Design Modifications

A comparative assessment of the overall performance of single-leaf sandwich door when the frame is the subject of in-depth study and, therefore, thoroughly examined is presented in Table 2. This summary details the maximum temperature and displacements values observed for the unexposed hinges case. Since the door upper and lower corners displacements remain partially unaltered, the subsequent optimization analysis will primarily use the computed temperatures to evaluate the effectiveness of the proposed configurations.

Table 2. Overall thermal and structural results for optimized frame designs.

Case Study	Numerical Analysis	Temperature (°C)		Door Displacement (mm)	
		Door	Frame	Upper Corner	Lower Corner
Frame Material	Aluminium Alloy	890	920	97.5	93.3
	Stainless Steel	620	690	100.0	93.6
	Wood	420	420	101.0	93.4
Frame Geometry	Insulation up to the wall	387	403	101.5	92.8
	With a steel sheet	396	415	101.7	92.8
Insulating Placement	Zone 5a	386	395	101.5	92.7
	Zones 5 and 5a	387	400	101.7	93.2
	Zones 5a and 6	395	411	101.7	93.2
	Zones 1 and 6	393	411	101.7	93.2
	Zones 2, 3, 4 and 5a	389	406	101.6	92.8
	Zones 1, 2, 3, 4, 5 and 6	402	419	101.6	93.2
	Zones 1, 5a and 6	395	411	101.7	93.2
Insulating Materials	Rock Wool	386	395	101.5	92.7
	Calcium Silicate	387	403	101.5	92.7
	Plasterboard	387	406	101.5	92.7

 doi:10.20944/preprints202601.0047.v1

	Fibreglass	401	425	101.5	93.1
	Polyurethane Foam	389	407	101.5	92.7
	Ceramic Fibre	387	403	101.5	92.7

3.3.1. Evaluation of the Thermal Behavior

Given that the frame is the critical component, the influence of its material on the thermal response of the system was analyzed. Three materials were evaluated: aluminum alloy (original material), stainless steel, and wood. Thermal results, presented in Table 2, showed that the aluminum alloy displays the worst performance, reaching the highest temperatures both in the frame and in the door: 920 and 890 °C, respectively. On the other hand, stainless steel presents a significant improvement compared to the aluminum alloy, with a temperature of 690 °C recorded in the frame (25% reduction) and 620 °C in the door (30% reduction). Wood stands out for its superior thermal performance, as a maximum temperature of 420 °C was recorded in both the frame and the door, representing a temperature reduction of over 50% compared to the original aluminum alloy frame. In view of the results observed, the aluminum alloy is no longer a viable option for the frame. Thus, wood was selected as the material for the frame in the following simulations, as it demonstrated the most favorable thermal behavior. It is important to mention that while Meranti wood [25] was utilized in this study, any other wood exhibiting comparable properties and fire resistance could have been substituted.

Considering a wooden frame, the study of the influence of its geometry on the overall performance of the door-frame system followed, where the frame with the original metal sheet and the frame with insulation extending up to the wall, i.e., with greater thickness, were analyzed. In both cases, all cavities of the frame were filled with insulating material (Zones 1, 2, 3, 4, 5a and 6, according to Figure 8). Although very close, the insulation up to the wall exhibited slightly better thermal performance than the metal sheet, with the frame and door reaching 402 and 377 °C, respectively. This marginal advantage justifies the selection of a wooden frame with insulation extending up to the wall, as this more robust configuration offers an advantageous performance baseline for further optimizations.

Following the determination of the optimal frame material and geometry, the study proceeded with the assessment of the insulation placement. Several insulation positions were analyzed, based on the principle that any unfilled cavity is modeled as wood, therefore resulting in a solid frame configuration for that region. Thermal results (Table 2) highlight two configurations: insulation inside the thermal break (Zone 5a in Figure 8) and insulation only at the frame boundaries (Zones 1 and 6 in Figure 8). Regarding the frame temperature, it is observed that the maximum temperatures recorded for the frame with insulation inside the thermal break and for the frame with insulation at the boundaries are 394 and 410 °C, respectively. Therefore, even though there is only a difference of 4.1%, positioning the insulation inside the thermal break proves to be the most effective option.

With a thicker wooden frame (insulation reaching the wall) and insulation only inside the thermal break, it is necessary to determine which insulation material promotes improved thermal performance. The results presented in Table 2 highlighted three materials: rock wool, calcium silicate and ceramic fiber. Calcium silicate and ceramic fiber reached similar maximum temperatures for both doors (387 °C) and frame (403 °C). However, rock wool proved to be the most effective material, recording the lowest door and frame temperatures: 386 and 395°C, respectively. Given that rock wool consistently yields the lowest temperatures in both door and frame, it is selected as the most viable insulating material for the final optimized frame design.

Thus, upon achievement of the iterative optimization process for the fire door frame, it is concluded that the modifications to the frame technical characteristics promote a thermal performance improvement of 57.3% for the frame and 58.3% for the door, compared to the original fire door.

3.3.2. Evaluation of Structural Behavior

 doi:10.20944/preprints202601.0047.v1

Regarding the door structural behaviour evaluated by its upper and lower corners displacements, it was found that the deformation results follow the trend observed in the original door-frame simulation, with greater deformations occurring at the upper corner. However, as previously mentioned, displacements remained largely unaffected by the modifications applied to the frame throughout the entire optimization process with a slight increase of 3.5% in the upper corner displacement and a 0.43% reduction in the lower corner, when compared to the original door displacements. Thus, it is evident that the modifications performed on the frame do not significantly influence the door structural behaviour.

4. Conclusions

Demanding certification standards and growing competition in the market have implications on the technical characteristics of fire doors and, therefore, are the subject of thorough studies. Considering this, with the main purpose of this project being the optimization of a single-leaf sandwich fire door, a numerical model was developed to assess its thermal and structural response in the event of a fire. However, due to the lack of information about the furnace inlet and outlet, it was not possible to implement the CFD-FEM coupled approach. As a result, a one-way coupling FEM approach between transient thermal and transient structural using Ansys Mechanical was carried out.

For this study, a total of 19 tests were performed accounting for different materials and geometries. It was shown that the frame is the key element for the failure of the door-frame assembly, given that it reaches 925 °C after a 60-minute exposure to fire. With the frame pinpointed as the element leading to failure, the subsequent optimization process focused on its design.

Results demonstrated that at the material level, both the frame and insulating materials influenced the fire door behavior. In addition, on a geometric level, the frame geometry and the arrangement of the insulation inside also impacted the results. When analyzing the frame material, it was proved that the aluminum alloy is not a viable option. In contrast, it was observed that opting for a wooden frame the temperature in both frame and door lowered by 55% compared to the original material (aluminum alloy). Furthermore, it was observed that a more robust wooden frame, i.e., with a greater thickness proved advantageous when compared to the original fire door. Finally, regarding the best insulation placement and insulating material, results showed that the application of rock wool inside the thermal break of a wooden frame extended up to the wall led to a reduction of 57.3% and 58.3 % of the frame and door temperature, respectively. It is important to note that the frame optimization had a greater impact on the thermal response than on the structural response, given that the recorded displacements in the upper and lower corners of the door remained almost unchanged, indicating that the performed modifications were more effective at reducing temperature than at minimizing deformation.

Although the model provided valuable insights, it is important to recognize certain limitations. For instance, the effects of wood combustion were not considered in the simulations. Building on this research, several directions for future work are proposed. A simplification of the simulation model, and consequently an aspect for future improvement, is that the material properties were defined as fixed values, meaning they were not temperature dependent. This simplification was due to the simulated temperatures being very high, and since the materials were not fully characterized, there was no available information about their properties at these temperatures. In this sense, it will be relevant to determine the complete properties of the materials used, namely Halspan and phenolic, as well as the other materials used in the simulation process, through thermophysical characterization tests.

Author Contributions: Conceptualization, M.F., A.A., J.S.; Methodology, A.A., J.S., J.T.; Software: A.A., J.S.; Validation, M.F., A.A., J.S., S.T, J.T.; Formal analysis, M.F., A.A., J.S., N.R., S.T, J.T.; Investigation, A.A., J.S., J.T.; Re-sources, S.T., J.T; Data curation, J.S., J.T.; Writing—Original Draft Preparation, M.F., J.S., N.R., S.T, J.T.;

 doi:10.20944/preprints202601.0047.v1

Writing—Review and Editing, M.F., J.S., S.T, J.T..; Visualization, M.F., A.A., J.S.; Supervision, S.T., J.S, J.T.; Project Administration, J.T.; All authors have read and agreed to the published version of the manuscript.

Funding: This research received no external funding.

Data Availability Statement: Data is contained within the article.

Acknowledgments: This work was supported by HAKEN WELT, LDA, I.P. by project scope UIBD/EMS/04077/2020 (METRICS) and by project scope UID/CEC/00319/2020 (ALGORITMI).

Conflicts of Interest: The authors declare no conflicts of interest.

Abbreviations

The following abbreviations are used in this manuscript:

CFD	Computational Fluid Dynamics
FEA	Finite Element Analysis
FEM	Finite Element Method

References

1. Strategies for Retrofitting an Existing Building to Meet the New Fire Code in Dubai.; May 15 2018.
2. Lim, B.; Bae, B.; Jang, M.; Lee, H.; Lee, C.; Kim, M.; Yi, C. Analysis of Fire Resistance Performance of Double Swing Fire Doors Using Thermo-Mechanical Model Depending on Gap Size. *Fire* **2025**, *8*, 238, doi:10.3390/fire8060238.
3. Izydorczyk, D.; Sędłak, B.; Papis, B.; Turkowski, P. Doors with Specific Fire Resistance Class. *Procedia Eng* **2017**, *172*, 417–425, doi:10.1016/j.proeng.2017.02.010.
4. Araújo, A.; Silva, J.; Teixeira, S.; Teixeira, J. Certification of a Fire Door – An Overview. In *Innovations in Industrial Engineering IV*; In Proceedings of ICIE 2025, 2025; pp. 279–289.
5. European Commitee for Standardization I.S.EN 1634-1:2014+A1:2018 - Fire Resistance and Smoke Control Tests for Door and Shutter Assemblies, Openable Windows and Elements of Building Hardware - Part1:Fire Resistance Test for Door and Shutter Assemblies and Openable Windows. 2018.
6. European Commitee for Standardization EN 13501-2:2007+A1 - Fire Classification of Construction Products and Building Elements - Part 2: Classification Using Data from Fire Resistance Tests, Excluding Ventilation Services. 2009.
7. Boscariol, P.; De Bona, F.; Gasparetto, A.; A. H. Kiaeian Moosavi, S.; Moro, L. Thermal Analysis of Fire Doors for Naval Applications . *PRADS2013* **2013**, 451–456.
8. Boscariol, P.; De Bona, F.; Gasparetto, A.; Moro, L. Thermo-Mechanical Analysis of a Fire Door for Naval Applications. *J Fire Sci* **2015**, *33*, 142–156, doi:10.1177/0734904114564955.
9. Kyaw Oo D'Amore, G.; Marinò, A.; Kašpar, J. Numerical Modeling of Fire Resistance Test as a Tool to Design Lightweight Marine Fire Doors: A Preliminary Study. *J Mar Sci Eng* **2020**, *8*, 520, doi:10.3390/jmse8070520.
10. Kyaw Oo D'Amore, G.; Mauro, F.; Marinò, A.; Caniato, M.; Kašpar, J. Towards the Use of Novel Materials in Shipbuilding: Assessing Thermal Performances of Fire-Doors by Self-Consistent Numerical Modelling. *Applied Sciences* **2020**, *10*, 5736, doi:10.3390/app10175736.
11. Kim, Y.U.; Chang, S.J.; Lee, Y.-J.; No, H.; Choi, G.S.; Kim, S. Evaluation of the Applicability of High Insulation Fire Door with Vacuum Insulation Panels: Experimental Results from Fire Resistance, Airtightness, and Condensation Tests. *Journal of Building Engineering* **2021**, *43*, 102800, doi:10.1016/j.jobe.2021.102800.
12. Khalifa, M.A.; Aziz, M.A.; Hamza, M.; Abdo, S.; Gaheen, O.A. Improvement of Fire Door Design Using Experimental and Numerical Modelling Investigations. *Journal of Structural Fire Engineering* **2022**, *13*, 205–223, doi:10.1108/JSFE-07-2021-0048.
13. Leung, H.Y.; Tam, H.K.; Tam, L.M.; Lao, S.K. CFD Analysis of the Heat Transfer of Fire Doors under the Standard Time-Temperature Curve. *ICCM2017* **2017**.

 doi:10.20944/preprints202601.0047.v1

14. Tlili, O.; Mhiri, H.; Bournot, P. Empirical Correlation Derived by CFD Simulation on Heat Source Location and Ventilation Flow Rate in a Fire Room. *Energy Build* **2016**, *122*, 80–88, doi:10.1016/j.enbuild.2016.04.028.
15. Iya, A.E.; Epée, A.F.; Mvogo, P.O.; Zaida, J.T.; Mouangue, R. Modelling and Numerical Simulation of a Compartment Fire: Flow Rate Behaviour at Opening. *Fire* **2023**, *6*, 185, doi:10.3390/fire6050185.
16. Prieler, R.; Ortner, B.; Pfeifer, T.; Kitzmüller, P.; Thumser, S.; Schwabegger, G.; Hochenauer, C. Fire Resistance of Gypsum-Sheathed Stud Walls with an Embedded Steel Door: Validation of a Numerical Approach. *Fire Saf J* **2023**, *141*, 103922, doi:10.1016/j.firesaf.2023.103922.
17. Prieler, R.; Langbauer, R.; Gerhardter, H.; Kitzmüller, P.; Thumser, S.; Schwabegger, G.; Hochenauer, C. Modelling Approach to Predict the Fire-Related Heat Transfer in Porous Gypsum Based on Multi-Phase Simulations Including Water Vapour Transport, Phase Change and Radiative Heat Transfer. *Appl Therm Eng* **2022**, *206*, 118013, doi:10.1016/j.applthermaleng.2021.118013.
18. Prieler, R.; Mayrhofer, M.; Eichhorn-Gruber, M.; Schwabegger, G.; Hochenauer, C. Development of a Numerical Approach Based on Coupled CFD/FEM Analysis for Virtual Fire Resistance Tests—Part A: Thermal Analysis of the Gas Phase Combustion and Different Test Specimens. *Fire Mater* **2019**, *43*, 34–50, doi:10.1002/fam.2666.
19. Prieler, R.; Gerhardter, H.; Landfahrer, M.; Gaber, C.; Schluckner, C.; Eichhorn-Gruber, M.; Schwabegger, G.; Hochenauer, C. Development of a Numerically Efficient Approach Based on Coupled CFD/FEM Analysis for Virtual Fire Resistance Tests—Part B: Deformation Process of a Steel Structure. *Fire Mater* **2020**, *44*, 704–723, doi:10.1002/fam.2846.
20. de Boer, J.G.G.M.; Hofmeyer, H.; Maljaars, J.; van Herpen, R.A.P. Two-Way Coupled CFD Fire and Thermomechanical FE Analyses of a Self-Supporting Sandwich Panel Façade System. *Fire Saf J* **2019**, *105*, 154–168, doi:10.1016/j.firesaf.2019.02.011.
21. Duthinh, D.; McGrattan, K.; Khaskia, A. Recent Advances in Fire–Structure Analysis. *Fire Saf J* **2008**, *43*, 161–167, doi:10.1016/j.firesaf.2007.06.006.
22. Ansys Theory Reference Manual - 6.1. Heat Flow Fundamentals Available online: https://ansyshelp.ansys.com/public/account/secured?returnurl=/Views/Secured/corp/v242/en/ans_thry/thy_heat1.html (accessed on 8 August 2025).
23. Byju's The Principle of Virtual Work Available online: https://byjus.com/gate/principle-of-virtual-work/#:~:text=The%20Principle%20of%20Virtual%20Work%20forms%20the,virtual%20displacements%20and%20evaluating%20the%20virtual%20work. (accessed on 30 July 2025).
24. Ansys Theory Reference Manual - 2.2. Derivation of Structural Matrices Available online: https://www.mm.bme.hu/~gyebro/files/ans_help_v182/ans_thry/thy_str2.html (accessed on 30 July 2025).
25. Leung, H.Y.; Tam, H.K.; Tam, L.M. CFD Analysis of the Heat Transfer of Fire Doors under the Standard Time-Temperature Curv. In Proceedings of the 8th International Conference on Computational Methods (ICCM2017); Guilin, Guangxi, China, 2017.